DOI: 10.24996/ijs.2022.63.12.11

ISSN: 0067-2904

Spectroscopic and Thermal Properties for Exploding Silver Wire Plasma in Deionized Water

Fatimah Jumaah Moaen*, Hammad R. Humud
Department of Physics, College of Science, University of Baghdad, Baghdad, Iraq

Received: 16/12/2021 Accepted: 23/2/2022 Published: 30/12/2022

Abstract
The goal of this research is to use optical emission spectroscopy to investigate the parameters of exploding silver wire plasma. The silver discharge plasma's emission spectra were recorded and studied. For silver wire of diameter 0.4 mm and different currents 75,100, and 125A in deionized water, the plasma electron temperature (T_e) was calculated by Boltzmann plot and container plasma medium temperature by thermal camera, and the electron density (n_e) was computed by Stark broadening using the hydrogen (H line) at 656.279 nm With increasing current from 75 to 125 A, the electron density (n_e) increased from 3.160×10^{17} to 8.762×10^{17} cm^{-3}, while electron temperatures increased from 0.571 to 1.334 eV under the same conditions. The plasma's optical emission spectrum (OES) includes a peak at 653 nm that corresponds to the H line of the hydrogen atom, as well as additional peaks that belong to Ag (AgI and AgII lines). Researchers looked into the relationship between plasma electron temperature, emission line intensity, and number density. Nanoparticle concentration rises as the intensity of the emission line rises, while their size decreases. It is feasible to deduce that plasma parameters have a regulated relationship with the concentration and size of nanoparticles produced.

Keywords: Exploding wire, Spectroscopy, Boltzmann plot, thermal camera, plasma characteristics.

الخصائص الطيفية والحرارية لتفجير بلازما الأسلاك الفضية في الماء منزوع الأيونات

فاطمة جمعة موين*, حمد رحيم حمود
قسم الفيزياء , كلية العلوم ,جامعة بغداد, بغداد ,العراق

الخلاصة
الهدف من هذا البحث هو استخدام التحليل الطيفي للانبعاثات الضوئية لفحص معاملات انفجار بلازما الأسلاك الفضية. تم تسجيل ودراسة أطياف انبعاث بلازما التفريغ الفضي بالنسبة للسلك الفضي بقطر(0.4mm) وتيارات مختلفة (100,75A و 125) في الماء منزوع الأيونات ، تم حساب درجة حرارة إلكترون البلازما (T_e) بواسطة طريقة بولتزمان ودرجة حرارة البلازما الحاوية المتوسطة بواسطة الكاميرا الحرارية ، وتم حساب كثافة الإلكترون (n_e) بواسطة توسع ستارك للسلك باستخدام الهيدروجين (H line)عند 656.279 نانومتر. وجد أن كثافة الإلكترون (n_e) تزداد من(cm^{-3} 3.160×10^{17} إلى 8.762×10^{17})مع زيادة التيار من 75 إلى A125 ، بينما تزداد درجات حرارة الإلكترون من (0.571ev إلى 1.334) لنفس الشروط.

*Email: fatimmalgaese@yahoo.com

يتميز طيف الانبعاث البصري (OES) للبلازما بقمة عند 653 نانومتر تتوافق مع خط H لذرة الهيدروجين ، بالإضافة إلى قمم أخرى تنتمي إلى Ag (خطوط AgI و AgII). تم فحص العلاقة بين درجة حرارة الإلكترون في البلازما وشدة خط الانبعاث والكثافة . يرتفع تركيز الجسيمات النانوية مع ارتفاع شدة خط الانبعاث ، بينما يقل حجمها. من الممكن استنتاج أن معلمات البلازما لها علاقة منظمة بتركيز وحجم الجسيمات النانوية المنتجة.

Introduction

The Electrical Explosion of Wires (EEW) is a process in which a metal wire is blown apart by a high-density current (>10^{10} A/m^2). Electromagnetic radiation, scattering products, and shock waves are all part of the process[1]. When particular conditions are met, the material of the wire is transformed into nanosized particles[2]. The EEW process includes steps such as solid state metal heating, melting, heating of fluid metal before commencing vaporization, wire material expansion, primary product dispersion, and final particle production[3]. During a rapid explosion, a metal wire enters a non-equilibrium state, defined by two forms of non-equilibrium: phase and temperature non-equilibrium. A metal wire is destroyed when an electric current is passed across it; the electronic subsystem is excited (to a temperature of 10^6K), the atomic subsystem, on the other hand, is cooler (10^4K). The major results of phase nonequilibrium include vapor (clusters), plasma, and overheated liquid drops[4][5]. Plasma is created by exploding wires with high electric energy and then passing it through various environments in a short period of time. Voltage, current pulse, material type and wire dimension, as well as the medium in which the explosion happens, are all controlled in the process of exploding wires[6][7]. One of the methods for diagnosing plasma is optical emission spectroscopy. It is used to collect information on plasma's nature, chemical compositions and plasma species, plasma density, and electron temperature are only a few examples[8].

Experimental Section

1-The Electric Exploding Wire technique

The nanoparticles were made in 30ml deionized water in an anti-shock container. Figure 1 shows how the preparation system works. Pure Ag wire (0.4 mm diameter) of 99.9 purity is exploded with an Ag plate with a power supply of high current (type edon – model MMA-300S/ China, work 50-300 A) at 80 V relative to the wire and dc currents of 75, 100, and 125 A to make the nanoparticles. Two electrodes were used, one in the shape of a wire and the other in the form of a plate. When a high current density travels across the electrodes, the two electrodes melt, evaporate, and convert into plasma, causing a shock wave in the surrounding medium due to its supersonic velocity. When plasma interacts with the surrounding gas or liquid, it cools, and nanoparticles form due to the nucleation process. Higher energy deposition in the wire, sufficient expansion volume, and speedy cooling of the particles are thought to be three criteria for the explosion wire in a liquid medium to create smaller particles.

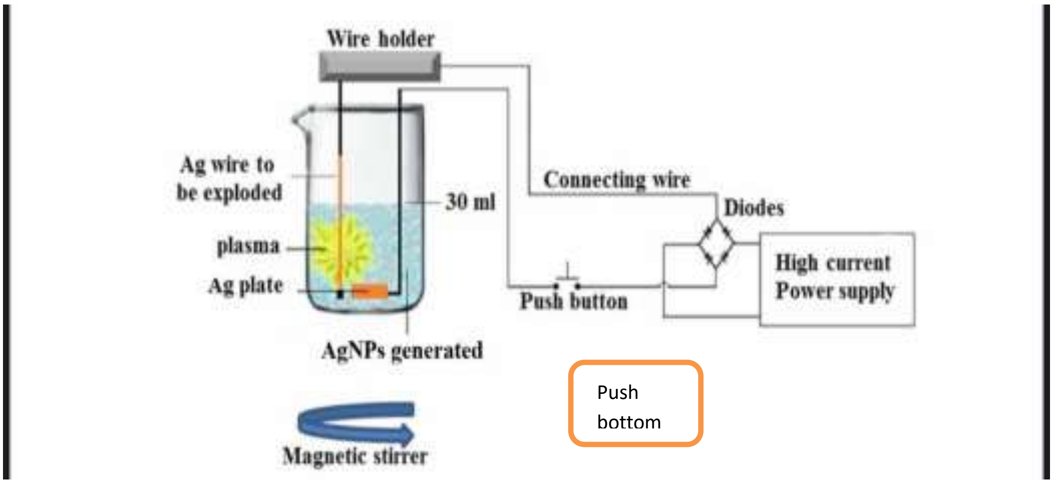

Figure 1: A diagram for EEW technique

2-Thermal properties

An imbalanced plasma is referred to as non-thermal plasma. In this plasma, the temperature of the electron is 10^4 times higher than that of the neutral gas[9]. Light and dynamic particles (electrons) combine to generate a chemically reactive medium in this fashion. Thermal damage to the surroundings is minimized by keeping the gas in the room at slightly increased temperatures [10].

3- Characterization Techniques

A thermal camera type S / N 90002261140 was used, as shown in Figure 2

Figure 2: Thermal camera.

The principle of operation of the camera is to track the desired body temperature[11]. The thermal imaging camera features a special lens that allows infrared radiation to pass through and strike the focused light, as well as a sensor that scans the data and pulls data from thousands of locations. As a result of this process, the field of view is known as a complicated temperature pattern. The process of creating a heat plan takes more than a few seconds to complete. The thermal drawing is subsequently turned into electrical impulses and transferred to the pulse of the signal processing unit, which turns the data into files. The visual data is represented by a color spectrum that corresponds to the amount of infrared energy emitted by the combination.

Figure 3: A diagram showing the parts of the thermal camera.

A spectrometer is an instrument which is used to analyze light over a specific portion of the electromagnetic spectrum, typically used in spectroscopic analysis to identify materials. The determination of wavelength emitted from plasma is very important for plasma diagnostics. The analysis is made by using the emission wavelength and intensity of the emission line at response time and it must be the same in every shot. For this purpose, a spectrometer model (HR 4000 CG-UV-NIR from Ocean Optics) was used in our setup to determine emission wavelengths. The spectrometer has a high resolution depending on the grating used in it and its high response material to wavelengths between (150 – 1000) nm with 3648 pixels.

Result and discussion

1- Optical emission spectroscopy results

Figure 4 depicts the optical emission spectrum (OES) emitted by plasma formed by exploding silver wire with a diameter of 0.4 mm with various currents (75,100,125 A). The peak at 656 nm corresponds to the H line for hydrogen atoms created by water molecule dissociation, as shown in the diagram, the other peaks belong to AgI and AgII peak intensities. It can be noted that the intensities increase as the current increases. This result agrees with that of Wankhede et al. [12].

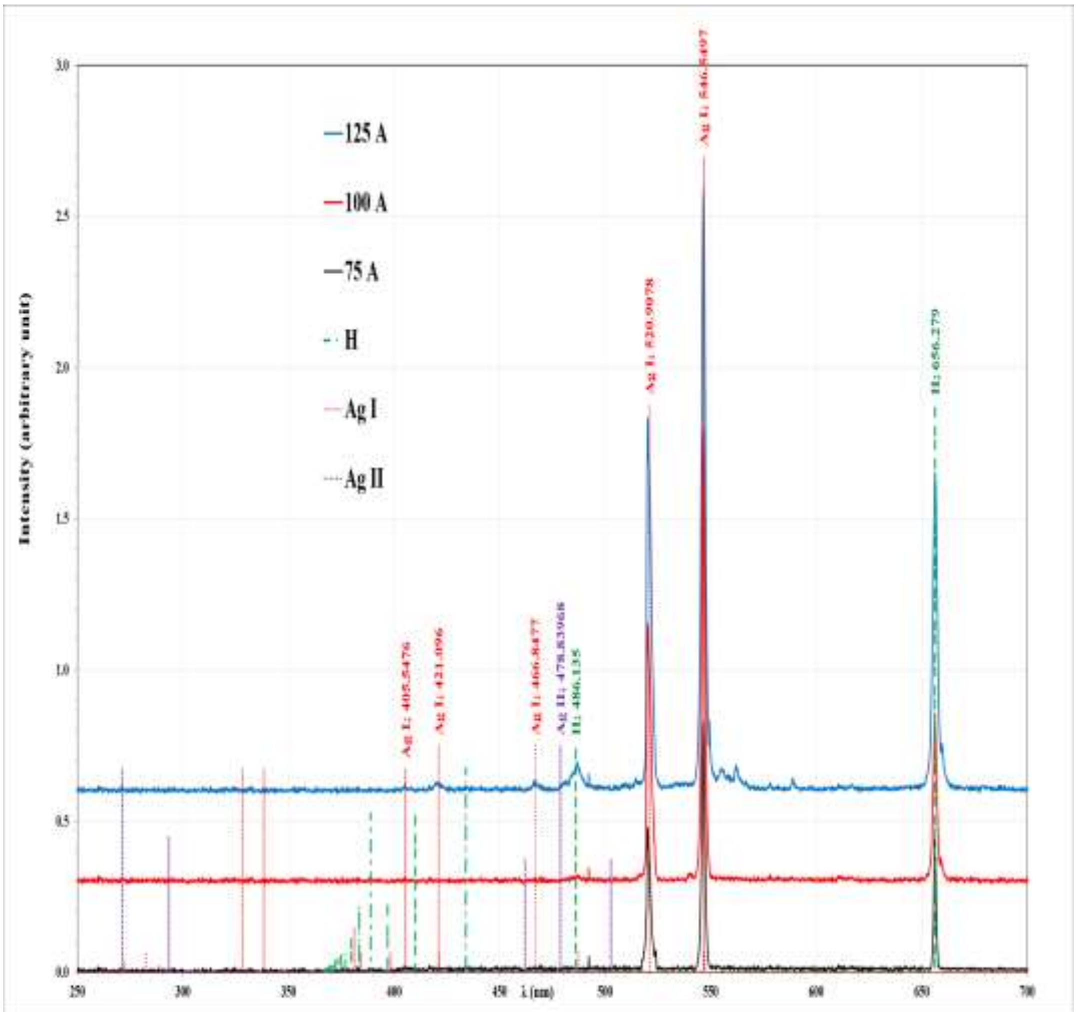

Figure 4: Emission spectra of Ag exploding wire at various currents of 75, 100, and 125 A.

The Boltzmann relation may be used to compute the electron temperature of plasma[13]:

$$Ln\left[\frac{\lambda_{ji}\, I_{ji}}{hcA_{ji}g_j}\right] = -\frac{1}{KT}\left(E_j\right) + ln\left|\frac{N}{U(T)}\right|$$

Where: λji, is the wavelength that corresponds to level j and level i transmission , *U(T)* is the partition function, N is the number of levels, g_j is the density of states, Ej is the energy at the highest level, Aji is the probability of transition between upper (j) and lower level transition states (i) and Te is the electron temperature . The electron temperatures (T_e) were determined from the slope of the best linear fit in the Boltzmann plot. Boltzmann plot requires peaks that originates from the same atomic species and the same ionization stage with Agl lines at (520.9078 and 546.5497nm) as shown in Figure 5 and the energies of upper levels, statistical weights, and transition probabilities used for the experimental plots for each element were obtained from the National Institute of Standard Technology database (NIST)[14]. The electron temperature equals the invert of the slope of the fitting line(the slope of the fitted line equals -1/k_B T) [15].

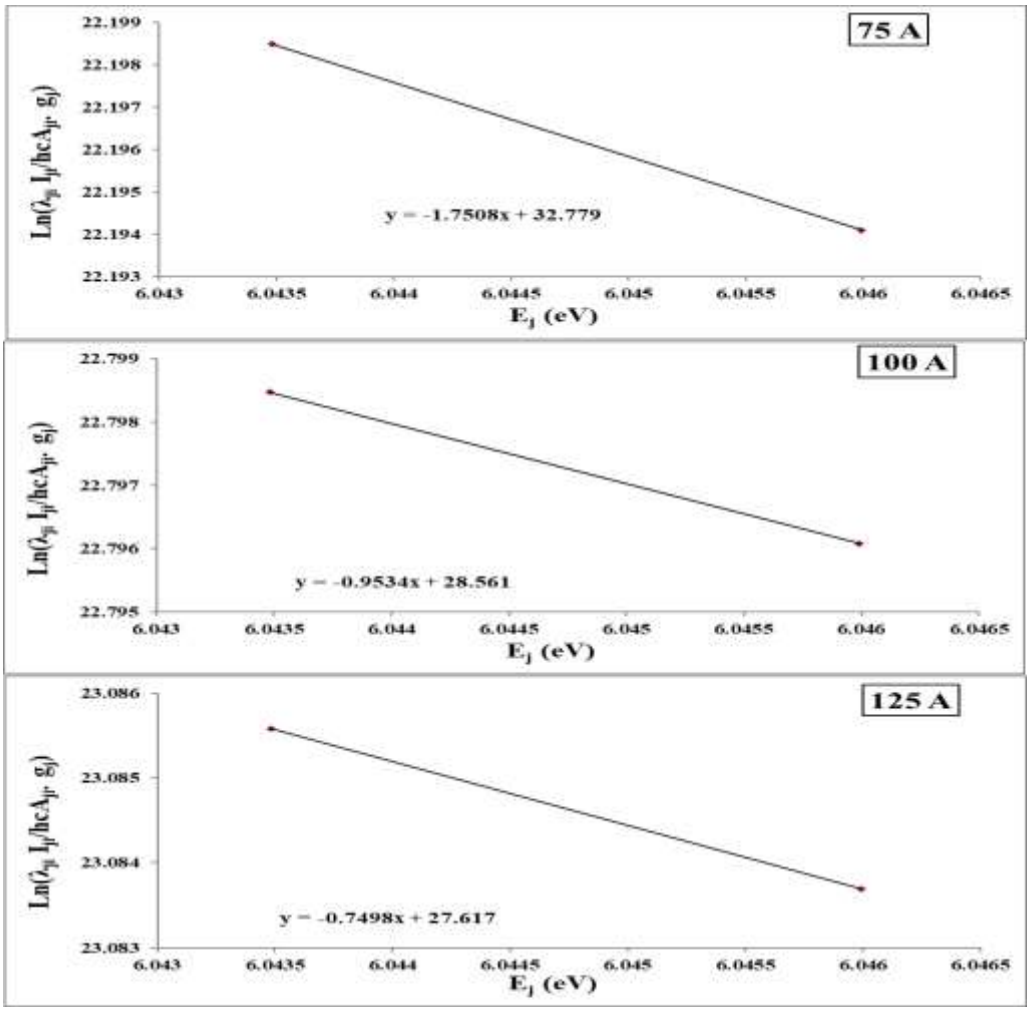

Figure 5: Boltzmann plot of AgI lines created by exploding wire at various currents

The electrons density was calculated using the stark broadening relation [16]:

$$\boldsymbol{n_e} = \left[\frac{\Delta\lambda}{2\omega_s}\right] \boldsymbol{N_r}$$

Where: $\boldsymbol{\Delta\lambda}$ is the line's FWHM and s is the electron impact parameter, both of which can be found in standard tables, and Nr is the reference electron density which equal 10^{16} (cm^{-3}) for neural atoms and $10^{17}(cm^{-3})$ for singly charged ions.

The peak profile of the 56.279 nm silver line is shown in Figure 6. Gaussian fitting was used to determine the entire width at half maximum The measured width depends on the Stark effect and the standard line width which is equal to 0.901nm, for the different samples. As the current increases, the full width widens, indicating an increase in electron density [17].

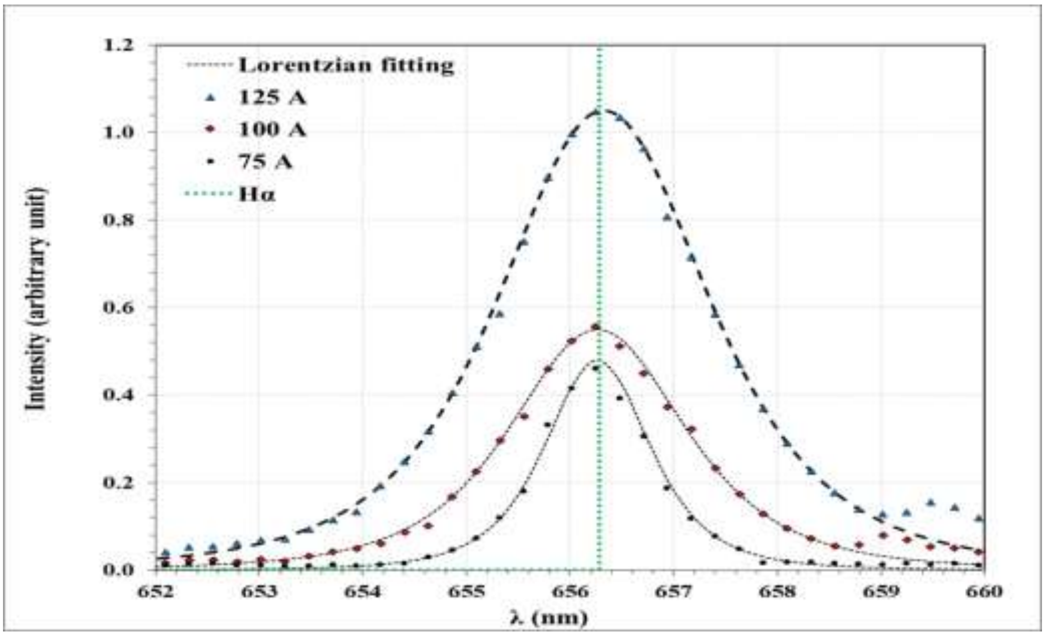

Figure 6: H broadens to 656.279 nm, and there is Gaussian fitting using various currents.

With different currents, the Boltzmann plot and the Stark broadening effect were used to quantify the variability in electron temperature (T_e) and electron density (n_e) .When the current was increased from 75 to 125 A, n_e increased from 3.160x10^{17} to 8.762x10^{17} cm^{-3}, while electrons' temperature rises from 0.571 to 1.334 eV. This result agrees with that of Wankhede et al. [12]. The decrease in concentration causes a decrease of collisions, which leads to an increase in electron temperature, which is lost in a variety of ways (collisions including elastic, excitation, and ionization)

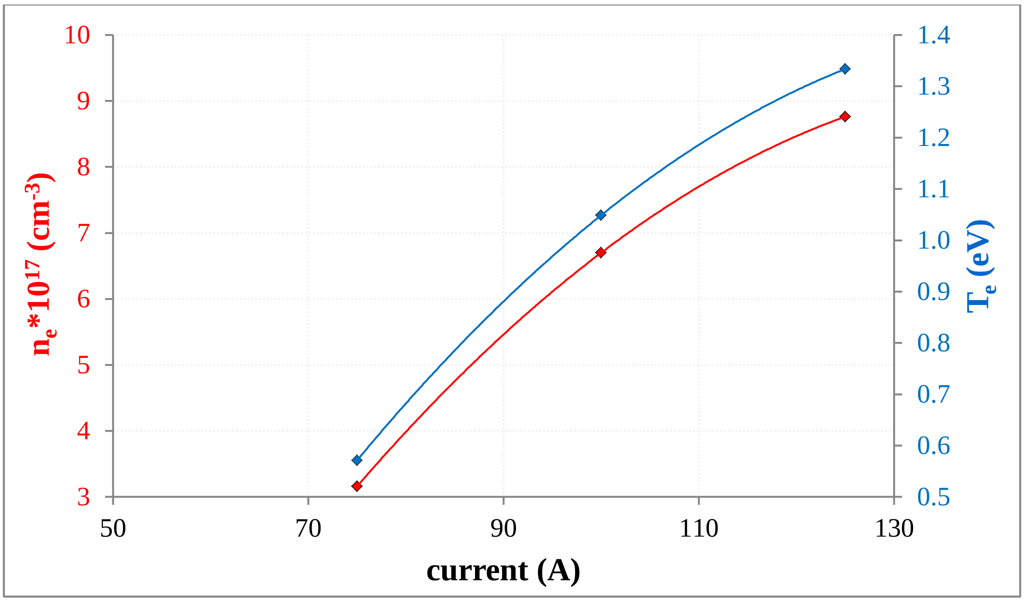

Figure 7: Electrons' temperature At varying currents, the Te and ne electron density for plasma created by a silver exploding wire.

Many parameters are used to characterize plasma, including the Debye length (λ_D), which is determined as follows[18]:

$$\lambda_{D=} \left[\frac{\varepsilon_o K_B T_e}{n_e e^2}\right]^{1/2} \cong 7.43x10^2\ cm$$

Where: *Te* and *ne* are the electron temperature and electron density, respectively. Plasma frequency can be calculated as[18][19]:

$$\omega_{pe=}(n_e e^2/m_e\varepsilon_0)^{\frac{1}{2}}\ Hz$$

The electric constant is ε_0, the electron mass is m_e, the electron number density is n_e, and the electron charge is e.
Table 1 shows the calculated Debye length (λ_D), plasma frequency (f_p), and Debye number (N_d) for silver plasma produced by exploding wires at currents of 57,100 and 125A.

Table 1: Plasma parameters for silver bursting wire with varied currents of 57, 100, and 125A computed from spectroscopic lines.

Current A	Te (eV)	FWHM (nm)	n_e*10^{17} (cm^{-3})	f_p (Hz) *10^{12}	λ_D*10^6(cm)	N_d
75	0.571	1.200	3.160	5.048	0.999	3
100	1.049	2.000	6.700	7.351	0.930	5
125	1.334	2.400	8.762	8.406	0.917	7

Description of the thermal characterization

Imaging with a thermal camera revealed the system's thermal nature, and the thermal distribution of the plasma results using EEW, as shown in Figure 8.

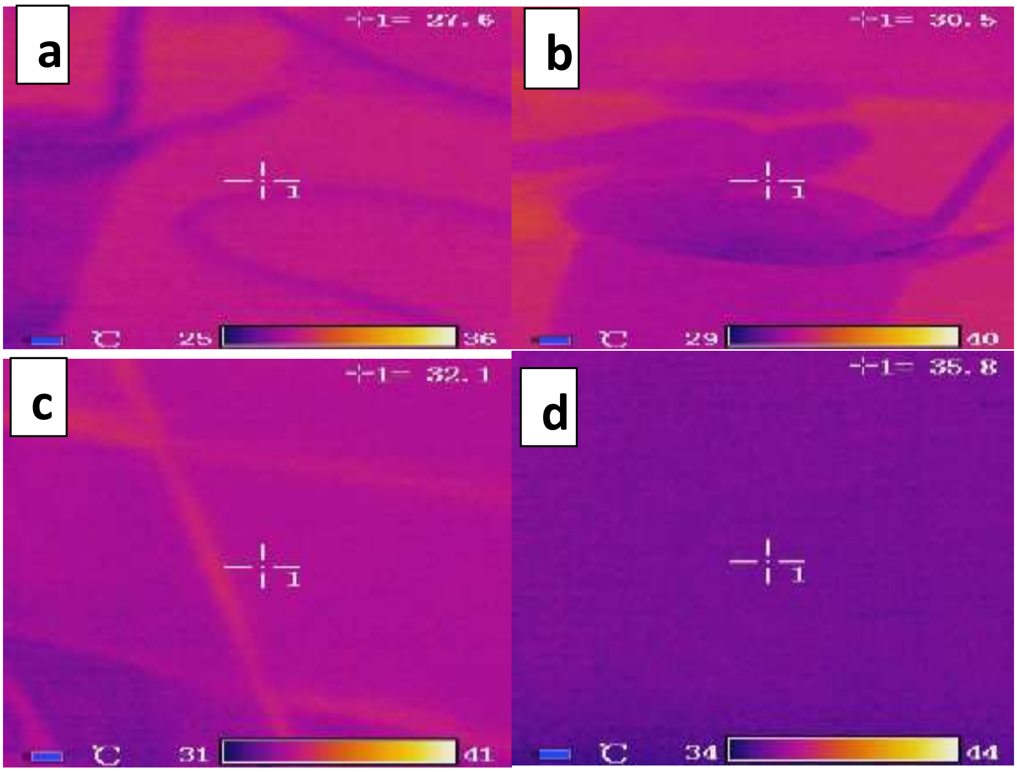

Figure 8: Thermal camera images for different currents of (a) 0mA (b)75mA (c) 100mA and(d) 125mA

The captured thermal images show the intensity of the heat distribution, where the temperature increases with the increase of the current. When the electrons move through the conductor, the electrons collide with the atoms of the conductor and lose some of their energy, which is converted into thermal energy. This was noticed in the form of an increase in the temperature of the conductor.

Table 2: Result of container medium plasma temperature using different currents

Current A	Temperature (^{O}C)
75	30.5
100	32.1
125	35.8

Conclusions

The following are some of the findings from this research of the effect of currents on spectra for produced emissions and plasma properties in the exploding wire technique:

• There were multiple atomic and ionic silver peaks in all spectra, as well as a conspicuous peak that matched the H line.

• Peak intensities grow as the current is raised, and as the input energy is increased.

• The electron density and temperature increase as the current increases.

•Despite the generation of high-temperature plasma because it is a pulsed degree and the temperature was measured in a short time, but it did not rise much from the ambient temperature because the reactants did not affect their physical properties with the ambient temperature.

Reference

[1] F.G.Hamzah and H.R.Humud, "Raspberry-Like Plasmonic Nanostructures Fabricated by Electrical Exploding Wire Technique for Raman Scattering Enhancement," *In AIP Conference Proceedings* ,vol. 22909,no.1, pp. 050033 ,2020

[2] Y. S. Kwon, Y. H. Jung, N. A. Yavorovsky, A. P. Illyn, & J. S. Kim, "Ultra-fine powder by wire explosion method," *Scripta materialia*, vol. 44, no. 8, pp.2247-2252, 2001.

[3] S. H. Abdullah, "Effect of current intensity on structural properties of cupper iodine nanoparticles produced by exploding Cu wire," *Iraqi Journal of Physics*, vol. 17, no. 41, pp. 1-6 ,2019.

[4] M. Krinitcyn, N. Toropkov, A. Pervikov, E. Glazkova, & M. Lerner, "Characterization of nano/micro bimodal 316L SS powder obtained by electrical explosion of wire for feedstock application in powder injection molding," *Powder Technology*, vol. 394, pp. 225-233, 2021.

[5] E. M.Abdelkader, P. A. Jelliss, & S. W. Buckner, "Main group nanoparticle synthesis using electrical explosion of wires," *Nano-Structures & Nano-Objects*, vol. 7, pp. 23-31, 2016.

[6] P. Wankhede, P. K. Sharma, & A. K. Jha, "Synthesis of copper nanoparticles through wire explosion route". J. Eng. Res. and Appl, vol. 3, no. 6, pp.1664-1669, 2013.

[7] A. Alqudami, S. Annapoorni, & S. M. Shivaprasad, "Ag–Au alloy nanoparticles prepared by electro-exploding wire technique," *Journal of Nanoparticle Research*, vol. 10, no. 6, pp.1027-1036, 2008.

[8] H. R. Humud, "Optical emission spectroscopy for studying the exploding copper wire plasma parameters in distilled water," *Iraqi Journal of Physics (IJP)*, vol. 15, no. 35, pp.142-147, 2017.

[9] M. Gruntman, E. C Roelof, D. G. Mitchell, H. J. Fahr, H. O. Funsten, & D.J. McComas, " Energetic neutral atom imaging of the heliospheric boundary region," *Journal of Geophysical Research: Space Physics*, vol.106, no. A8, pp.15767-15781, 2001.

[10] S. Iwanaga, E. S. Toberer, A. LaLonde, & G. J. A. Snyder, "high temperature apparatus for measurement of the Seebeck coefficient," *Review of Scientific Instruments*, vol. 82, no. 6, pp.063905, 2011.

[11] M. J. Alwazzan, "Low cost blood vein detection system based on near-infrared LEDs and image-processing techniques," *Polish Journal of Medical Physics and Engineering*, vol. 26, no. 2, pp.

61-67, 2020.

[12] P. Wankhede, P. K.Sharma, A. K. JHA, "Synthesis of copper nanoparticles through wire explosion route," *J. Eng. Res. and Appl*, vol. 3, no. 6, pp. 1664-1669, 2013.

[13] Y. Ralchenko, J. R. Fuhr, F. C. Jou, A. E. Kramida, W. C. Martin, L. I. Podobedova, & W. L. Wiese, "New Generation of the NIST Atomic Spectroscopic Databases," *In AIP Conference Proceedings*, vol.771, no.1, pp. 276-285, 2005.

[14] "NIST National Institute of Standards and Technology USA, electronic database."

[15] J. E. Sansonetti and W. C. Martin, Am. Inst. Phys., 34 (2005) 1-6., vol. 242, pp. 93–163, 1996.

[16] N. M. Shaikh, S. Hafeez, B. Rashid, & M. A. Baig "Spectroscopic studies of laser induced aluminum plasma using fundamental, second and third harmonics of a Nd: YAG laser," *The European Physical Journal D*, vol. 44, no.2, pp. 371-379, 2007.

[17] N. Konjević, A. Lesage, J. R. Fuhr, & Wiese, W. L. "Experimental Stark widths and shifts for spectral lines of neutral and ionized atoms," *Journal of Physical and Chemical Reference Data*, vol. 31, no. 3, pp. 819-927, 2002

[18] H. Hashim, "Spectroscopic Diagnostics of Exploding Aluminum Wire Plasma in Distilled Water," *Al-Nahrain Journal of Science*, vol. 21, no. 2, pp. 88-91, 2018.

[19] INAN, Umran S. GOŁKOWSKI, "*Marek. Principles of plasma physics for engineers and scientists". Cambridge University Press*, pp. 10-13,2010.